Small x PDFs at HERA: Inclusive, Unintegrated, Diffractive

Victor Lendermann[†]
Kirchhoff-Institut für Physik, Universität Heidelberg, Im Neuenheimer Feld 227, 69120 Heidelberg, Germany

Abstract
The present status of HERA measurements of the proton parton distribution functions (PDFs) in the low x domain is presented. PDFs extracted from DIS ep data within the standard factorisation ansatz, as well as unintegrated PDFs and those describing the diffractive component of the ep scattering cross section are discussed.

1 Inclusive Analyses

1.1 Combination of H1 and ZEUS Data

Deep inelastic scattering cross sections measured at HERA provide the major input for the determination of the proton structure at low x. Using the standard QCD factorisation ansatz, the parton distribution functions are extracted from the doubly differential neutral (NC) and charge (CC) current cross sections measured as a function of the Bjorken x and of the four-momentum transfer squared Q^2. Over the past two decades, global fit procedures have been developed which determine the quark and gluon PDFs of the proton using QCD DGLAP evolution equations at increasingly higher orders of perturbation theory (see [1] for an overview). The QCD fits are applied to data sets from a number of different experiments and consider correlations among the experimental data points.

This traditional extraction procedure however has certain drawbacks in the treatment of systematic uncertainties. In particular, correlations through common systematic uncertainties, both within and across data sets, represent a significant challenge. The treatment of these correlations is not unique. In the Hessian method [2], each systematic error source is treated as an additional fit parameter, and the parameters are fitted assuming the model, as provided by (N)NLO QCD, to optimise the uncertainties and to constrain the PDFs. In the Offset method (see *e.g.* [3,4]) the data sets are shifted by the effect of each single systematic error source before fitting, and the resulting fits are then used to form an envelope function as an estimate of the PDF uncertainty. All analyses face the problem of data sets not always leading to consistent results. Some global QCD analyses therefore inflate the PDF uncertainties.

The drawbacks mentioned can be significantly reduced by averaging the cross section data from the different data sets in a model independent way prior to performing a QCD analysis. The H1 and ZEUS collaborations presented preliminary results of combining their HERA I data [5], where one averaged value of the cross section is provided for each measured kinematic point at a given (x, Q^2, y). Using a method introduced in Ref. [6], the correlated systematic uncertainties are floated coherently allowing each experiment to calibrate the other. This reduces significantly

[†] On behalf of the H1 and ZEUS Collaborations

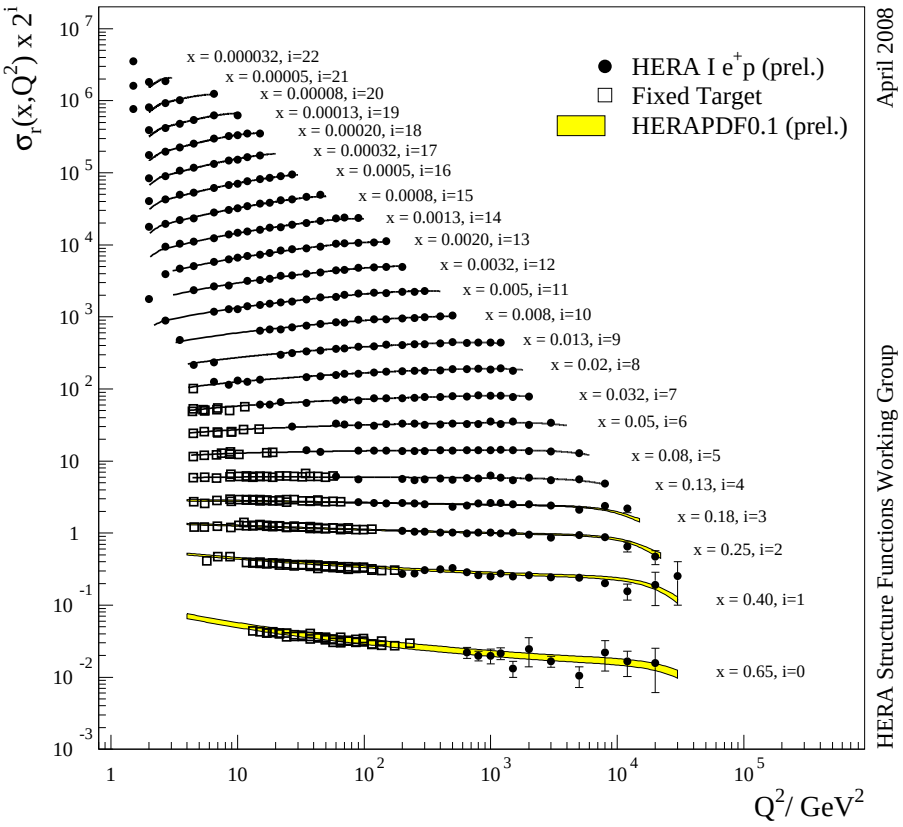

Fig. 1: DIS NC e^+p scattering cross section from the HERA I data taking period as obtained by combining the published H1 and ZEUS measurements. The predictions of the HERAPDF 0.1 fit are superimposed.

the correlated uncertainties for much of the kinematic plane. In addition, a study of the global χ^2/ndf of the average and of the pull distributions provides a model independent consistency check between the experiments.

Prior to the combination, the H1 and ZEUS data were transformed to a common grid of (x, Q^2) points using ratios of cross sections calculated based on available PDF parameterisations. The NC and CC data collected with the proton beam energy of $E_p = 820$ GeV were corrected to 920 GeV and then combined with the measurements at $E_p = 920$ GeV.

As an example, the resulting NC e^+p cross section data are shown in Fig. 1. A precision better than 2% is reached in the low Q^2 region. Comparisons with the fits previously performed by H1 and ZEUS to their own data have shown an excellent agreement.

At the time of this workshop, H1 presented preliminary results of the analysis of their HERA I e^+p data collected in 1999-2000 in the range $12 \leq Q^2 \leq 150\,\text{GeV}^2$ and $2 \cdot 10^4 \leq x \leq 0.1$. The data have been combined with the previously published H1 data in this region using a similar averaging procedure. The accuracy of the combined measurement is typically in the range of 1.5 – 2%.

1.2 PDF Fit of the Combined HERA Data

The H1/ZEUS combined data set has been used as the sole input for a new NLO DGLAP PDF fit [7]. The consistency of the input data enables a calculation of the experimental uncertainties of the PDFs using the χ^2 tolerance, $\Delta\chi^2 = 1$. This represents a significant advantage compared to the global fit analyses using both HERA and fixed target data, where increased tolerances $\Delta\chi^2 = 50 - 100$ are used to account for data inconsistencies. Other advantages of using solely HERA data are: the absence of heavy target corrections which must be applied to the ν-Fe and μD fixed target data, and no need to assume isospin symmetry, *i.e.* that d distribution in the proton is the same as u distribution in the neutron.

For the new HERAPDF 0.1 fit, the importance of correlated systematic uncertainties is no longer crucial, since they are relatively small. This ensures that similar results are obtained using either Offset or Hessian method, or by simply combining statistical and systematic uncertainties in quadrature.

A DGLAP PDF fit analysis depends on a number of model parameters, like the choice of the starting scale Q_0^2 for the evolution, the form of the x dependence for PDFs at the starting scale, the minimum Q^2 for the data to fit, $Q^2_{\rm min}$, the treatment of heavy flavours etc. There are differences in the choices made by different groups, and in particular, by H1 and ZEUS in their fits to their own data. In this analysis, both collaborations agreed on a common set of choices, and variations in the choices were taken to estimate model-dependent uncertainties (see [7] for details).

The predictions of the fit for the NC cross section are superimposed in Fig. 1 on the combined HERA NC data set. The yellow band shows the total uncertainty including those due to the model dependency. The total uncertainties of the HERAPDF 0.1 PDFs are much reduced compared to the PDFs extracted from the analyses of the separate H1 and ZEUS data sets, as can be seen in Fig. 2, where the new PDFs are compared to the ZEUS-JETs and H1PDF2000 PDFs.

1.3 Measurements of F_L

At high inelasticities $y = Q^2/(xs)$, where s is the ep centre-of-mass energy squared, the inclusive DIS cross section is sensitive to the size of the structure function F_L which describes the exchange of longitudinally polarised bosons. In the Quark Parton Model F_L is zero, since due to helicity and angular momentum conservation a quark with spin $\frac{1}{2}$ cannot absorb a longitudinally polarised photon [8]. In QCD, F_L differs from zero, receiving contributions from quarks and from gluons [9]. At low x (which corresponds to high y) the gluon contribution greatly exceeds the quark contribution. Therefore F_L is a direct measure of the gluon distribution to a very good approximation. An independent measurement of F_L at HERA, and its comparison with predictions derived from the gluon distribution extracted from the DGLAP fits, thus represents a crucial test on the validity of perturbative QCD at low x. Furthermore, depending on the particular theoretical approach adopted, whether it be a fixed order pQCD calculation, a re-summation scheme, or a colour dipole ansatz, there appear to be significant differences in the predicted magnitude of F_L at low Q^2 mainly due to a large uncertainty of the gluon PDF. A measurement of F_L may be able to distinguish between these approaches.

A direct measurement of F_L requires several sets of data taken at the same x and Q^2 but

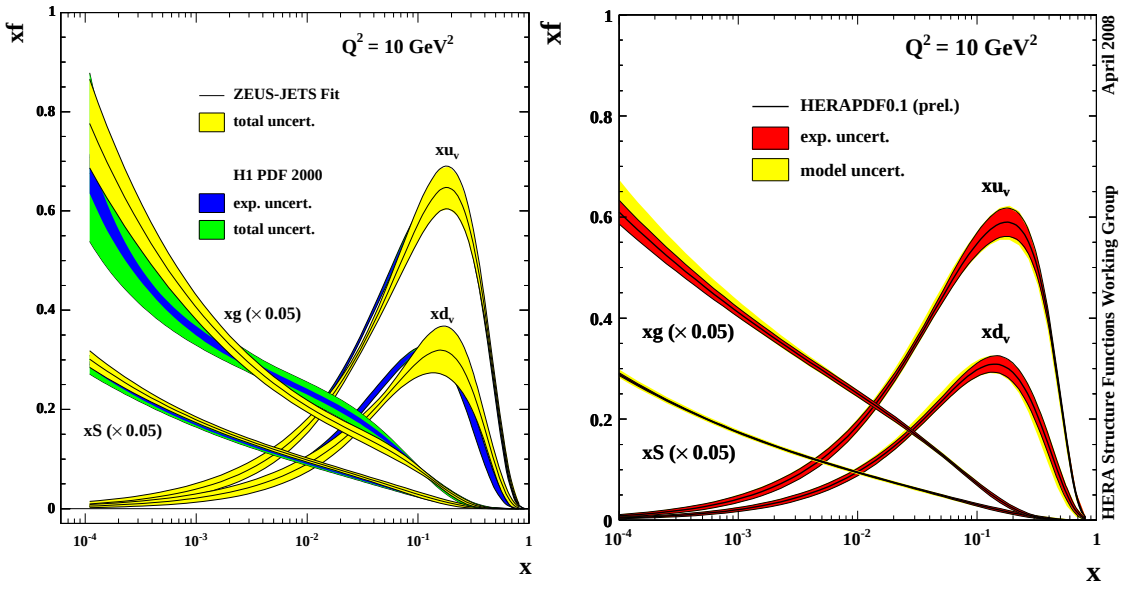

Fig. 2: Left: PDFs from the ZEUS-JETS and H1PDF2000 fits. Right: HERAPDF 0.1 PDFs from the analysis of the combined data set.

with different y values. Due to the relationship $y = Q^2/xs$ this requires data to be collected at different centre-of-mass energies, which was done in the last year of HERA running, when dedicated runs were performed with lowered proton beam energies of $E_p = 460$ and 575 GeV.

The first HERA measurement of $F_L(x, Q^2)$ was reported by H1 [10] in the range $12 \leq Q^2 \leq 90\,\mathrm{GeV}^2$ and $0.0002 \leq x \leq 0.004$. In this analysis, the scattered electron is reconstructed in the H1 backward calorimeter SpaCal. Preliminary results were presented by ZEUS in a similar kinematic range [11]. Both measurements show a non-zero F_L and are consistent with each other and with the prediction of (N)NLO QCD fits. Further preliminary results were presented by H1 in an extended range of Q^2 up to $800\,\mathrm{GeV}^2$, where the scattered electron is found either in the SpaCal or in the Liquid Argon calorimeter covering the central and forward region of the H1 detector [12]. These results are shown in Fig. 3.

2 Unintegrated PDFs

Using the QCD factorisation theorem, PDFs extracted from DIS data are applied for the calculation of various scattering processes at hadron colliders, in particular at the LHC. In practice, the interpretation of experimental data relies for many signals on analytical calculations performed at a fixed order of perturbation theory, typically NLO or NNLO (see [13] for a recent review), as well as on Monte Carlo (MC) event simulations. The major MC programs, PYTHIA [14] and HERWIG [15], include leading order matrix elements for a number of processes, while effects of higher orders of pQCD are simulated using parton shower models.

For some signatures, especially those with high multiplicity of final state objects, the complex kinematics and the large phase space available at high energies to be reached at the LHC

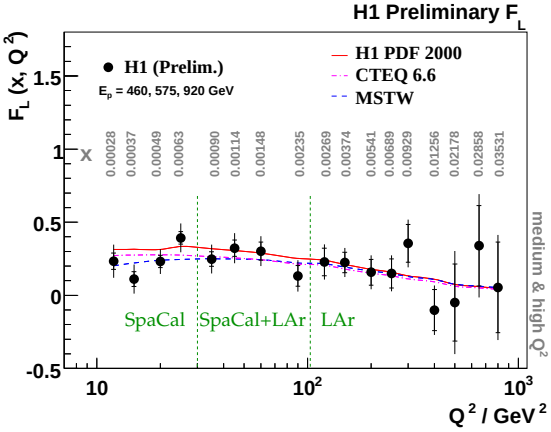

Fig. 3: Preliminary results of the H1 measurement of the proton structure function F_L shown as a function of Q^2 at the given values of x. The inner error bars denote the statistical error, the full error bars include the uncorrelated systematic errors. The solid curve describes the expectation on F_L from the H1 PDF 2000 fit using NLO QCD. The dashed (dashed-dotted) curve depicts the expectation of the MSTW (CTEQ) group using NNLO (NLO) QCD. The theory curves connect predictions at the given (x, Q^2) values by linear extrapolation.

make them potentially sensitive to effects of QCD initial state radiation arising from the tail of finite transverse momenta k_T of partonic distributions. In perturbative fixed-order calculations finite-k_T contributions are partially accounted for. This is usually sufficient for inclusive cross sections, but likely not for more exclusive final state observables. As an illustration, Fig. 4 (left) from an H1 study of D^*+jet photoproduction at HERA [16] shows the cross section for this process as a function of the difference in the azimuthal angle $\Delta\phi(D^*, \text{jet})$ between the D^* and the jet. The lower $\Delta\phi$ tail is significantly underestimated by the analytical NLO programs FMNR [17,18] and ZMVFNS [19, 20].

On the other hand, the standard MC programs are based on collinear evolution of the initial state partons, supplemented by colour coherence effects for soft gluon emission. It is unknown whether the approximations involved in these methods will provide sufficient precision at the LHC energies, as the effects of not collinearly ordered emissions become increasingly important at low x. A theoretical framework including the finite-k_T contributions makes use of generalised QCD factorisation technique which involves PDFs unintegrated not only in the longitudinal but also in the transverse momenta [21] and couples them with suitably defined off-shell matrix elements. Although MC generators based on this framework [22–25] are generally not as developed as the standard parton shower programs, several studies have demonstrated their potential advantages over collinear approaches for specific hadronic final states. This is illustrated in Fig. 4 (right) in which the same distribution of the azimuthal angle difference $\Delta\phi(D^*, \text{jet})$ from the H1 study [16] is compared to the prediction of the MC program CASCADE [22]. A good agreement with the data is observed in the whole angular range.

Another example is shown in Fig. 5 in which the azimuthal separation between the two leading jets $\delta\phi$ is plotted for dijet and three-jet production studied by ZEUS in DIS at HERA [26] and compared to HERWIG and CASCADE predictions [27]. CASCADE is superior to HERWIG both in the normalisation and in the shape of the distribution.

3 Diffractive PDFs

A significant fraction, of the order of 10%, of DIS events at HERA are characterised by a large rapidity gap between hadrons found in the main detector and the hadronic remnant escaping

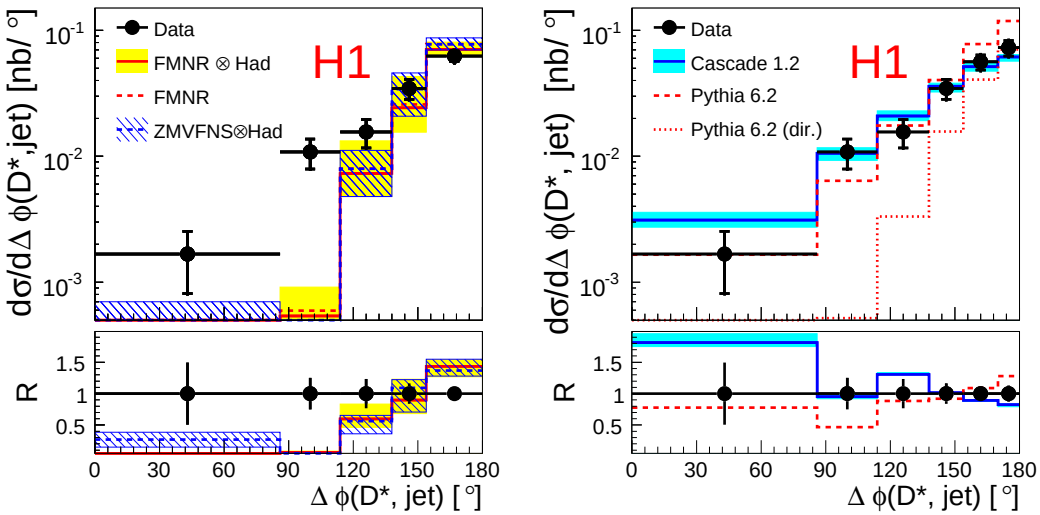

Fig. 4: D^*+jet cross section as a function of $\Delta\phi(D^*, \text{jet})$ measured by H1 in photoproduction at HERA and compared with the prediction of the next-to-leading order calculations FMNR and ZMVFNS on the left and of the MC generators PYTHIA and CASCADE on the right.

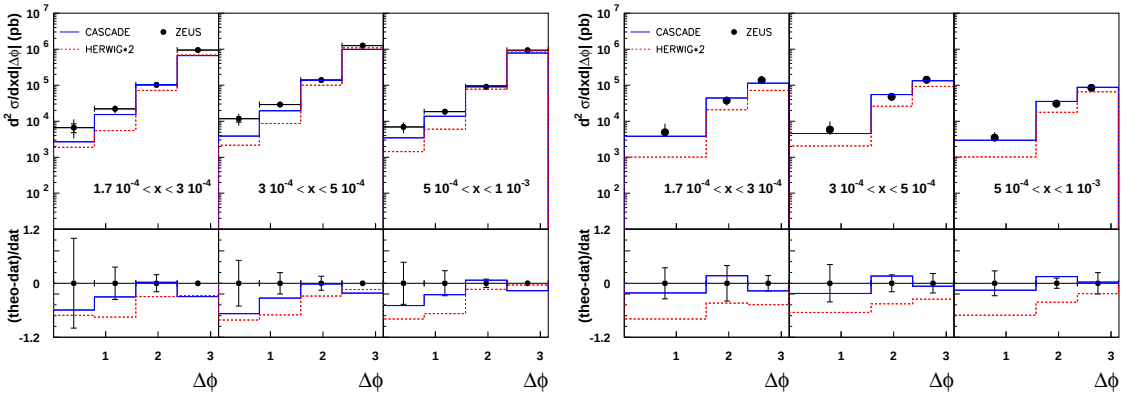

Fig. 5: Dijet (left) and three-jet (right) production cross section measured by ZEUS in DIS at HERA as a function of the azimuthal angle $\Delta\phi$ between the two leading jets in different x intervals and compared to the prediction of HERWIG and CASCADE.

through the forward beam pipe. Inclusive diffractive processes are analysed employing various techniques: *(i)* explicitly selecting events with a large rapidity gap; *(ii)* extracting the diffractive contribution from a fit to the invariant mass M_X of the reconstructed hadronic system; *(iii)* tagging the scattered proton in the dedicated forward spectrometers located far away from the main detectors and very close to the beam pipe (FPS in H1, LPS in ZEUS) and vetoing the proton dissociation. The different analyses are based on different statistics and are characterised by different systematic effects. All H1 and ZEUS analyses are broadly consistent within the quoted uncertainties, and the possibility of creating combined H1-ZEUS data sets, similar to the inclusive HERA data, is currently being considered.

Diffractive events at HERA are successfully described within the Regge framework [28], in which the rapidity gap is explained by the exchange of a colourless object lying on the Pomeron trajectory. The description of the cross section is based on a two-step factorisation approach. The first step is the standard QCD factorisation, describing the cross section as a convolution of the matrix element for the hard scale boson-quark interaction with a PDF in the proton. The second step describes the PDF as a product of the universal Pomeron flux in the proton with the diffractive PDF (DPDF). The Pomeron flux is described by the respective trajectory and depends solely on the fraction of the proton momentum carried by the Pomeron $x_{I\!P}$ and the four-momentum transfer squared at the proton vertex t. The DPDF provides, at a given Q^2, the parton content of the Pomeron for a given longitudinal momentum fraction $\beta = x/x_{I\!P}$ carried by the struck quark. Additionally, a small additional term in the second factorisation describes the Reggeon exchange component.

The second factorisation is an empirical assumption which is not proven theoretically. Various experimental studies at HERA have shown this ansatz to work to a good approximation. However, a recent ZEUS study [29] revealed violation of this factorisation, as shown in Fig. 6. Looking in particular at the $x_{I\!P}$ intervals in the central column, one observes a clear change in the Q^2 slope of the structure function $x_{I\!P}F_2^D(x_{I\!P}, \beta, Q^2)$ which is defined similarly to the conventional structure function F_2 in inclusive DIS. The effect is rather mild, as compared to the typical precision of the diffractive measurements, and thus should not strongly affect QCD analyses of diffractive PDFs which are based on this assumption.

The diffractive PDFs, defined in this framework, were extracted from inclusive diffractive data by H1 [30] in an NLO DGLAP QCD analysis. While the singlet quark distribution is well constrained by the fit, there is a significant uncertainty of the gluon distribution especially at high $z_{I\!P}$. Here, $z_{I\!P}$ is the longitudinal momentum fraction of the parton entering the hard sub-process with respect to the diffractive exchange, such that $z_{I\!P} = \beta$ for the lowest order quark-parton model process, whereas $0 < \beta < z_{I\!P}$ for higher order processes. An additional constraint was obtained from the analysis of diffractive dijet production in DIS at HERA [31]. The dijet data which are sensitive to the gluon distribution at high $z_{I\!P}$ have shown a remarkable consistency with the predictions from a fit of inclusive diffraction. Including these data into a combined analyses resulted in a set of the most precise diffractive PDFs currently available. Examples of the H1 2007 Jets DPDF fit predictions for the singlet quark and gluon diffractive PDFs at different factorisation scales μ_f^2 squared, where $\mu_f^2 = Q^2$ in inclusive diffraction, are shown in Fig. 7.

References

[1] R. Devenish and A. Cooper-Sarkar. Oxford, UK: Univ. Pr. (2004).

[2] C. Pascaud and F. Zomer. LAL-95-05;
C. Pascaud and F. Zomer (2001). hep-ph/0104013.

[3] H1 Collaboration, C. Adloff *et al.*, Eur. Phys. J. **C13**, 609 (2000). hep-ex/9908059.

[4] ZEUS Collaboration, S. Chekanov *et al.*, Eur. Phys. J. **C42**, 1 (2005). hep-ph/0503274.

[5] H1 Collaboration. Preliminary results, H1prelim-07-007;
ZEUS Collaboration. Preliminary results, ZEUS-prel-07-026.

[6] A. Glazov, AIP Conf. Proc. **792**, 237 (2005).

[7] H1 Collaboration. Preliminary results, H1prelim-08-045;
ZEUS Collaboration. Preliminary results, ZEUS-prel-08-003.

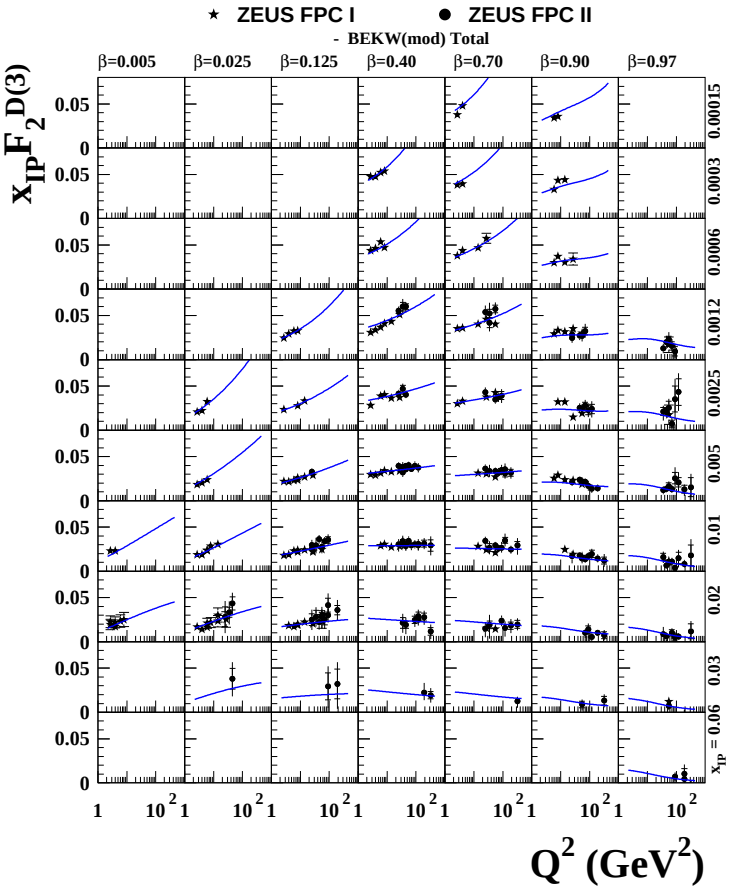

Fig. 6: The diffractive structure function of the proton $x_{I\!P} F_2^D(3)$, as a function of Q^2 for different regions of β and $x_{I\!P}$, as measured by ZEUS. The inner error bars show the statistical uncertainties and the full bars the statistical and systematic uncertainties added in quadrature. The curves show the result of a fit to the data based on a modified BEKW model [32].

[8] C. Callan and D. Gross, Phys. Rev. Lett. **22**, 156 (1969).

[9] F. W. A. Zee and B. T. S. Phys. Rev. D **10**, 2881 (1974);
G. Altarelli and G. Martinelli, Phys. Lett. B **76**, 89 (1978).

[10] H1 Collaboration, F. D. Aaron *et al.*, Phys. Lett. B **665**, 139 (2008). 0805.2809.

[11] ZEUS Collaboration. Preliminary results, ZEUS-prel-08-001.

[12] H1 Collaboration. Preliminary results, H1prelim-08-042.

[13] NLO Multileg Working Group Collaboration, Z. Bern *et al.* (2008). arXiv:0803.0494.

[14] T. Sjöstrand, S. Mrenna, and P. Skands, JHEP **05**, 026 (2006). hep-ph/0603175.

[15] G. Corcella *et al.*, JHEP **01**, 010 (2001). hep-ph/0011363;
G. Corcella *et al.* (2002). hep-ph/0210213.

[16] H1 Collaboration, A. Aktas *et al.*, Eur. Phys. J. C **50**, 251 (2007). hep-ex/0608042.

[17] S. Frixione, M. L. Mangano, P. Nason, and G. Ridolfi, Phys. Lett. B **348**, 633 (1995). hep-ph/9412348.

[18] S. Frixione, P. Nason, and G. Ridolfi, Nucl. Phys. B **454**, 3 (1995). hep-ph/9506226.

[19] B. A. Kniehl (2002). hep-ph/0211008.

[20] G. Heinrich and B. A. Kniehl, Phys. Rev. D **70**, 094035 (2004). hep-ph/0409303.

[21] S. Catani, M. Ciafaloni, and F. Hautmann, Phys. Lett. B **242**, 97 (1990);
S. Catani, M. Ciafaloni, and F. Hautmann, Nucl. Phys. B **366**, 135 (1991);
S. Catani, M. Ciafaloni, and F. Hautmann, Phys. Lett. B **307**, 147 (1993).

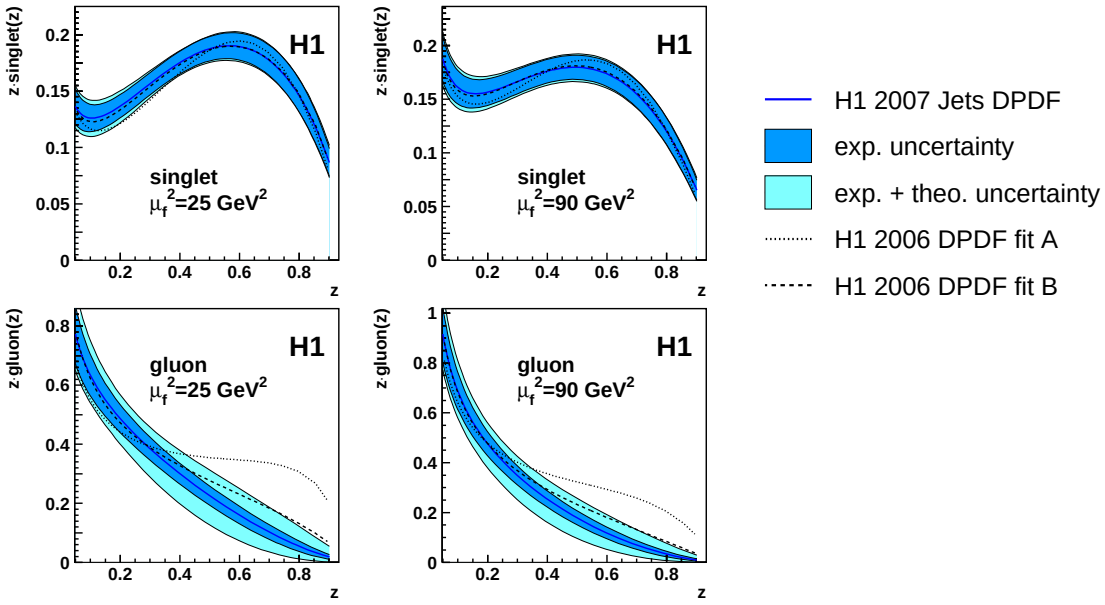

Fig. 7: The diffractive quark (top) and gluon (bottom) PDF as a function of $z_{I\!P}$ for two values of the squared factorisation scale μ_f^2: 25 GeV^2 (left) and 90 GeV^2 (right). The solid line indicates the H1 2007 Jets DPDF [31], surrounded by the experimental uncertainty (dark shaded band) and the experimental and theoretical uncertainties added in quadrature (ligh shaded band). The dotted and dashed lines show the DPDFs corresponding to the H1 2006 fits [30].

[22] H. Jung and G. P. Salam, Eur. Phys. J. C **19**, 351 (2001). hep-ph/0012143; H. Jung, Comput. Phys. Commun. **143**, 100 (2002). hep-ph/0109102.

[23] G. Gustafson, L. Lönnblad, and G. Miu, JHEP **09**, 005 (2002). hep-ph/0206195; L. Lönnblad and M. Sjodahl, JHEP **02**, 042 (2004). hep-ph/0311252; L. Lönnblad and M. Sjodahl, JHEP **05**, 038 (2005). hep-ph/0412111.

[24] K. J. Golec-Biernat, S. Jadach, W. Placzek, P. Stephens, and M. Skrzypek, Acta Phys. Polon. B **38**, 3149 (2007). hep-ph/0703317.

[25] S. Hoche, F. Krauss, and T. Teubner, Eur. Phys. J. C **58**, 17 (2008). arXiv:0705.4577.

[26] ZEUS Collaboration, S. Chekanov *et al.*, Nucl. Phys. B **786**, 152 (2007). arXiv:0705.1931.

[27] F. Hautmann and H. Jung, JHEP **10**, 113 (2008). arXiv:0805.1049.

[28] P. D. B. Collins. Cambridge 1977.

[29] ZEUS Collaboration, S. Chekanov, Nucl. Phys. B **800**, 1 (2008). 0802.3017.

[30] H1 Collaboration, A. Aktas *et al.*, Eur. Phys. J. C **48**, 715 (2006). hep-ex/0606004.

[31] H1 Collaboration, A. Aktas *et al.*, JHEP **10**, 042 (2007). 0708.3217.

[32] J. Bartels, J. R. Ellis, H. Kowalski, and M. Wusthoff, Eur. Phys. J. C **7**, 443 (1999). hep-ph/9803497.

Documents describing HERA preliminary results can be downloaded from the WWW sites:
H1: https://www-h1.desy.de/publications/H1preliminary.short_list.html
ZEUS: http://www-zeus.desy.de/public_results/publicsearch.html